Synthesis, structural studies and biological properties of new TBA analogues containing an acyclic nucleotide

Teresa Coppola [a], Michela Varra [a,*], Giorgia Oliviero [a], Aldo Galeone [a], Giuliana D'Isa [a], Luciano Mayol [a], Elena Morelli [b], Maria-Rosaria Bucci [c], Valentina Vellecco [c], Giuseppe Cirino [c], Nicola Borbone [a]

[a] Dipartimento di Chimica delle Sostanze Naturali, Università degli Studi di Napoli "Federico II", via D. Montesano 49, 80131 Napoli, Italy
[b] Dipartimento di Chimica Farmaceutica e Tossicologica, Università degli Studi di Napoli "Federico II", via D. Montesano 49, 80131 Napoli, Italy
[c] Dipartimento di Farmacologia Sperimentale, Università degli Studi di Napoli "Federico II", via D. Montesano 49, 80131 Napoli, Italy

ARTICLE INFO

ABSTRACT

A new modified acyclic nucleoside, namely N^1-(3-hydroxy-2-hydroxymethyl-2-methylpropyl)-thymidine, was synthesized and transformed into a building block useful for oligonucleotide (ON) automated synthesis. A series of modified thrombin binding aptamers (TBAs) in which the new acyclic nucleoside replaces, one at the time, the thymidine residues were then synthesized and characterized by UV, CD, MS, and ^{1}H NMR. The biological activity of the resulting TBAs was tested by Prothrombin Time assay (PT assay) and by purified fibrinogen clotting assay. From a structural point of view, nearly all the new TBA analogues show a similar behavior as the unmodified counterpart, being able to fold into a bimolecular or monomolecular quadruplex structure depending on the nature of monovalent cations (sodium or potassium) coordinated in the quadruplex core. From the comparison of structural and biological data, some important structure–activity relationships emerged, particularly when the modification involved the TT loops. In agreement with previous studies we found that the folding ability of TBA analogues is more affected by modifications involving positions 4 and 13, rather than positions 3 and 12. On the other hand, the highest anti-thrombin activities were detected for aptamers containing the modification at T13 or T12 positions, thus indicating that the effects produced by the introduction of the acyclic nucleoside on the biological activity are not tightly connected with structure stabilities. It is noteworthy that the modification at T7 produces an ON being more stable and active than the natural TBA.

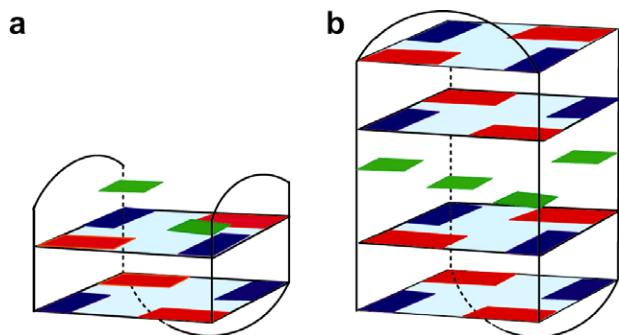© 2008 Elsevier Ltd. All rights reserved.

1. Introduction

Thrombin is a serine protease playing a central role in the clotting process; converting soluble fibrinogen to fibrin; activating the factors V, VIII, and XI; and stimulating platelet aggregation. A high number of bio-molecules bind this protein allowing the fine regulation of the clotting process thus preventing any loss of blood and avoiding inappropriate clots.[1] Alterations between procoagulant and anticoagulant stimuli are the bases of pathological diseases such as the formation of venous or arterial thrombi, the major causes of mortality in the western countries.[2–4] For these reasons, the development of anticoagulant strategies to inhibit thrombogenesis is currently of great interest and, among these, the most important are focused on direct or indirect inhibition of thrombin. In the latest years, direct thrombin inhibitors have undergone extensive studies in view of their potential anticoagulant properties since, differently from heparin, they do not bind to plasma proteins.[5] One of these direct inhibitors that specifically binds to human thrombin (EC$_{50}$ of 20 nM) is the TBA,[6–15] a 15-mer oligonucleotide identified in 1992 by SELEX technology[16,17] (Systematic Evolution of Ligands by EXponential enrichment). In vitro studies showed that TBA, used at nanomolar concentrations, prolongs clotting time from 25 to 43 s in human plasma.[6] Notwithstanding its in vivo half-life is 1–2 min, studies conducted on canine cardiopulmonary bypass showed that it is able to maintain extracorporeal circulation by employing a constant infusion.[18]

The solution-state three-dimensional structure of the TBA has been determined by NMR methods.[12–14,19,20] Feigon and co-workers[12] have evidenced that their NMR data fitted with both monomolecular and symmetrical intermolecular dimeric structure. On the basis of other NMR results produced by studying the folding of modified aptamers, they deduced that the tertiary structure of the TBA was intramolecular, so that, it is generally assumed that it adopts a chair-like structure consisting of two G-tetrads connected by two lateral TT loops and a central TGT loop (a, Fig. 1). After this work the intermolecular folding (b, Fig. 1) was not further investigated. However, Vorlicôva[21] and co-workers have recently demonstrated by CD analyses and EMSA experiments that the folding of TBA is bimolecular, putting new questions about

* Corresponding author. Tel.: +39 081678540; fax: +39 081678746.
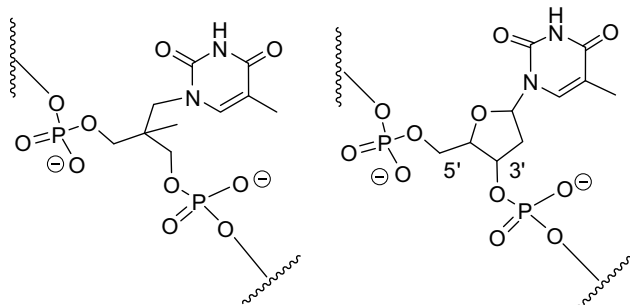E-mail address: varra@unina.it (M. Varra).

Figure 1. Schematic representation of TBA structures: (a) monomolecular quadruplex; (b) symmetrical bimolecular quadruplex. In both schematic representations red and blue squares indicate the G bases in *anti* and *syn* conformation, respectively. The green squares indicate the T4 and T13 bases bound to each other by a hydrogen bond and stacked on the adjacent G-quartet.

structure–activity relationships, which have been, until today, referred to the TBA-thrombin complex models fulfilled by NMR[12–14] and/or crystal[11,15] methods, in which the aptamer adopts the chair-like structure.

In light of literature data and with the aim to get new insight about the thrombin-TBA recognition, we have undertaken a study concerning the synthesis and the structural and biological characterization of a new series of modified TBA, in which the thymidines have been replaced, one at the time, by the acyclic nucleoside N^1-(3-hydroxy-2-hydroxymethyl-2-methylpropyl)-thymine (**T***, Fig. 2). Various modifications involving the loops have been brought on the TBA sequence, showing that, besides the G-quartets, they are involved in the recognition between thrombin and TBA.[22–25] Oligonucleotides (ONs) incorporating acyclic nucleotides are of current interest for many reasons. For example they are less susceptible to nuclease action in relation to natural counterpart.[26–28] The increasing interest toward these derivatives is also due to the hypothesis that oligonucleotides characterized by the replacement of all the sugar moieties by acyclic linkers could have represented the precursors of nucleic acids in probiotic times.[29] For these reasons a highest number of ONs containing acyclic nucleotide derivatives has been synthesized. In most of the cases a carbon atom of the ribose ring is lacking, thus achieving a structural simplification of the resulting molecules.

The structural changes between the acyclic and the unmodified T residue (Fig. 2) can be summarized as follows: (i) one bond shortening between T base and one phosphate group; (ii) the presence of an hydrophobic moiety, namely a methyl group; (iii) the presence of a prochiral carbon in the linker that develops into a chiral center when the modified nucleotide is inserted in the sequences. The ability of the synthesized sequences to assume a quadruplex conformation has been valued by NMR, UV, and CD spectroscopies.

Finally, their thrombin inhibitor activity has been evaluated by PT and purified fibrinogen clotting assays.

2. Results

2.1. Chemistry

The synthesis of acyclic T derivative phosphoramidite is reported in Scheme 1. The key reaction of the global synthesis is the Mitsunobu condensation[30,31] between 5-hydroxymethyl-2,2,5-trimethyl-1,3-dioxane (**1**) and N^3-benzoylthymine (**2**). To perform this reaction the linker and the base were first submitted to the pertinent protecting procedure.

The commercially available starting material 1,1,1-tris(hydroxymethyl)ethane was converted into 5-hydroxymethyl-2,2,5-trimethyl-1,3-dioxane (**1**) by reaction with 2,2-dimethoxypropane in the presence of pyridinium-*p*-toluene sulfonate as catalyst.

The selective protection of thymine base at N^3 position has been firstly obtained by the Reese[32] procedure. The latter consists in the conversion of thymine into N^1,N^3-dibenzoyl derivative by using benzoylchloride (2.2 equiv) and a mixture of acetonitrile-pyridine (5:2 v/v) as solvent; the resulting product was, in turn, hydrolyzed by a rapid treatment with a carbonate solution, to obtain the desired N^3-benzoylthymine. However this procedure gives rather poor yields with the recovery of a high quantity of unreacted starting material. In an effort to improve the yields, we found that by extending the time of the first reaction an increasing amount of N^3-benzoylthymine is achieved probably derived from the decomposition of the N^1,N^3-derivative. Higher yield for the N^3-benzoylthymine (**2**) was obtained by one step reaction, extending the treatment of thymine with benzoyl-chloride at 72–78 h.

The Mitsunobu reaction between **1** and **2** has been carried out by using triphenylphosphine, di-*tert*-butyl-azodicarboxylate as coupling agents and dioxane as solvent. The condensation product N^3-benzoyl-N^1-[(2,2,5-trimethyl-1,3-dioxan-5-yl)methyl]-thymine (**3**) was then treated with Dowex® 50W-X8(H$^+$) resin[33] obtaining N^3-benzoyl-N^1-[3-hydroxy-2-(hydroxymethyl)-2-methylpropyl]-thymine (**4**). The latter derivative has been characterized by mono-

Figure 2. Structural difference between the acyclic (left) and T (right) nucleotides.
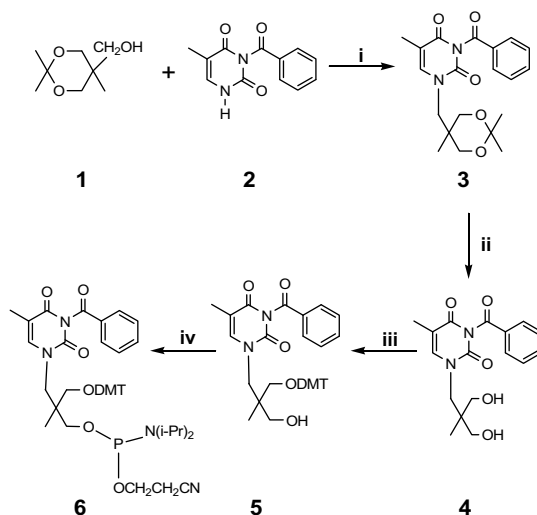
Scheme 1. Synthesis of acyclic nucleoside phosphoramidite. Reagents: (i) Mitsunobu condensation: **1** (9 mmol), **2** (4 mmol), PPh$_3$ (6 mmol), DtBAD (6 mmol), and dioxane (25 mL); (ii) **3** (10 mmol), DOWEX (30 mmol), and H$_2$O/CH$_3$OH (1/9 v/v, 50 mL); (iii) **4** (8 mmol), DMTCl (2 mmol), DMAP (0.4 mmol), and Py (32 mL); (iv) **5** (4 mmol), DIPEA (16 mmol), 2-cianoethyl-diisopropyl-chlorophosphoramidite (2 mmol), DCM (35 mL).

and bi-dimensional NMR spectroscopy experiments (^{1}H, ^{13}C, NOESY, and COSY) and mass spectrometry. The conversion of **4** in the phosphoramidite building block (**6**) has been achieved by using the standard procedure[34] (see Section 5). The monomer **6** was then successfully used for the synthesis of modified TBAs by an automated DNA synthesizer. The acyclic nucleoside has been inserted, one at the time, as a T mimic in each position of the loops (Table 1).

2.2. UV and CD experiments

The ability of all the TBA analogues to fold into an antiparallel quadruplex arrangement was tested by CD analyses. For each CD experiment, an ON concentration of 1×10^{-5} M was used. Two sets of experiments were obtained using one of the following buffers: 100 mM KCl, 10 mM KH$_2$PO$_4$, pH 7.4 (K buffer); 10 mM NaH$_2$PO$_4$, 2.7 mM KCl, 137 mM NaCl, pH 7.4 (phosphate-buffered saline, PBS). CD spectra have shown a profile very similar to that obtained for the natural TBA (**I**, Table 1) with positive and negative maxima at 295 and 265 nm, respectively, which are generally accepted as diagnostic for an antiparallel quadruplex arrangement.[35]

In order to assign, by CD analysis, the molecularity of the structures formed by the modified ONs, we have monitored the amplitude of CD positive band at 295 nm produced by each ON at different concentrations: 1×10^{-4}, 1×10^{-5}, and 1×10^{-6} M. It is well known that a monomolecular structure produces CD bands whose amplitude, expressed as molar ellipticity, is independent of the concentration.[21] All CD experiments registered at 10 °C in K buffer have shown a dependence of the molar ellipticity on the concentration, thus indicating that the folding is intermolecular for all the sequences (one example is reported in Fig. 3). However, the UV thermal analyses performed in the same buffer (Fig. 5b) have shown ambiguous profiles. For all species the experiments seem to indicate that two transitions occur, the first around 25–30 °C and the latter around 50 °C. To exclude that the dependence

of the molar ellipticity on the concentration was due to end-to-end interaction between two monomolecular quadruplexes, induced by the cooling procedure, the CD experiments were repeated at 30 °C. Unchanged results, besides a small diminution of molar ellipticity (Fig. 3c and inset d), have been checked confirming the intermolecular folding for all the ONs sequences. Surprisingly, invariability of molar ellipticity has been found using the physiological PBS (one example is reported in the Fig. 4) or a similar sodium phosphate buffer totally KCl free (data not shown). These data suggest that the TBA and its analogues opt for the inter- or intra-molecular folding according to the nature of the cations present in the solution. It is noteworthy that the physiological concentration of KCl present in PBS (2.7 mM) is insufficient to shift these structures from mono- to bimolecular forms.
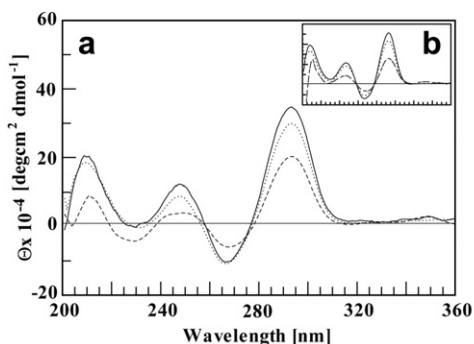
To evaluate the thermal stability[36–39] of the quadruplex folded structures of **I–VII** (Table 1), UV melting curves have been registered using a temperature interval scan from 10 to 80 °C at fixed wavelength (295 nm). Each experiment has been repeated at two different scan rates of 0.1 and 0.5 °C/min (not shown) in both PBS and K buffers (a and b, respectively, in Fig. 5). In all cases, changing the scan rate, no differences have been evidenced. Furthermore, all melting (from 10 to 80 °C) and folding (from 80 to 10 °C) profiles have not shown hysteresis phenomena.

The sequence-stability relationship data reported in Table 1 are in agreement with the structural model in which T9, T4, and T13 are stacked on the adjacent G-quartet with the latter two base paired to each other.[12–14] In fact, these types of interactions can be totally (as in the case of **V**) or partially (as in the cases of **III** and **VII**) disrupted by the introduction of the acyclic nucleotide at these positions. On the contrary, not unexpectedly, **II** and **VI** have shown no lowering of T_m values, while for **IV** a slight increase
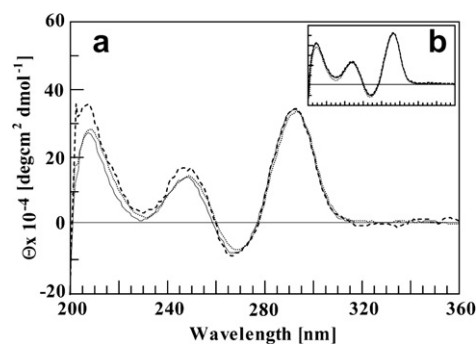
Table 1
UV melting temperatures of TBA and its analogues

| ON	Sequences	T_m (K buffer)	T_m (PBS)
I	GGTTGGTGTGGTTGG	50	33
II	GGT$_3$*TGGTGTGGTTGG	51	34
III	GGTT$_4$*GGTGTGGTTGG	47	30
IV	GGTTGGT$_7$*GTGGTTGG	54	37
V	GGTTGGTGT$_9$*GGTTGG	39	22
VI	GGTTGGTGTGGT$_{12}$*TGG	51	34
VII	GGTTGGTGTGGTT$_{13}$*GG	47	30

ON concentration: 1.0×10^{-5} M; K buffer: 100 mM KCl, 10 mM KH$_2$PO$_4$, pH 7.4; PBS: 137 mM NaCl, 2.7 mM KCl, 10 mM NaH$_2$PO$_4$, pH 7.4.

Figure 4. CD spectra of **VII** (a) and **I** (inset b) registered using physiological PBS (137 mM NaCl, 2.7 mM KCl, 10 mM NaH$_2$PO$_4$, and pH 7.4) at three ON concentrations: 1×10^{-4} M (solid line); 1×10^{-5} M (dotted line); 1×10^{-6} M (dashed line).
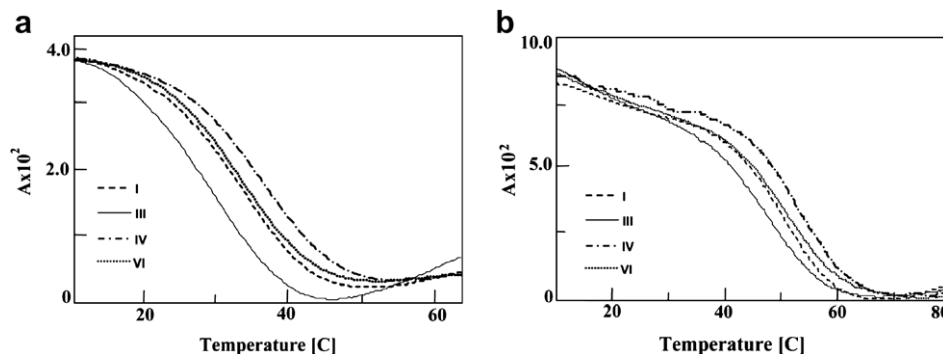

Figure 3. CD spectra at 10 and 30 °C of **VII** (a and c, respectively) and **I** (insets b and d, respectively) registered using potassium phosphate as dissolving buffer (100 mM KCl, 10 mM KH$_2$PO$_4$, and pH 7.4) at three ON concentrations: 1×10^{-4} M (solid line); 1×10^{-5} M (dotted line); 1×10^{-6} M (dashed line).
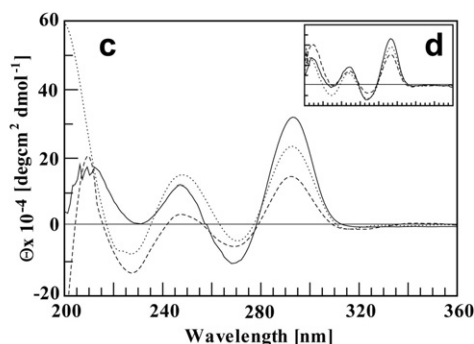
Figure 5. Normalized melting profile of **I**, **III**, **IV**, **VI**: (a) physiological PBS and (b) potassium phosphate buffer. The scan rate is fixed at 0.1 °C/min. T_m values are taken as minimum point of each curve derivative calculated using the corresponding function in the UV JASCO program. All T_m values are reported in Table 1.

in T_m value was observed, thus suggesting a marginal role of residues T3, T12, and T7 on the structural stability.

Finally, for all ONs, differential UV (Fig. 6) and CD spectra (Fig. 7) recorded at different temperatures have been carried out using physiological PBS. In all cases but **V**, the data evidenced isoelliptic and isosbestic points, thus indicating that only one typology of monomolecular quadruplex is present in solution.[21]

2.3. ^{1}H NMR experiments

The ^{1}H NMR spectrum of TBA is characterized by the presence of eight well-resolved signals in the 11.5–12.5 ppm region attributable to the exchange protected imino protons involved in the formation of Hoogsteen hydrogen bonds of two G tetrads. Moreover, in the aromatic region (6.8–8.5 ppm) fifteen proton signals attrib-

utable to H8 and H6 protons of guanine and thymine bases, respectively, are present.[12–14] By increasing the temperature the intensity of imino signals progressively decreases and, at the same time, the number of the aromatic resonances doubles due to the contemporaneous presence in solution of the two mutual exchanging folded and unfolded ONs (data not shown). Rising the temperature above 50 °C the disappearing of all imino protons signals takes place, and the number of aromatic signals drops back again to fifteen due to the exclusive presence in solution of the unfolded ON. Very similar signal patterns (for some examples see Fig. 8), as well as similar thermal behaviors, can be observed for the NMR spectra of all but **V** the modified TBAs, thus suggesting a comparable folding. In some cases, however, the ^{1}H NMR spectra appear more crowded due to the splitting of several proton signals. This finding can be confidently explained by considering that the substitution
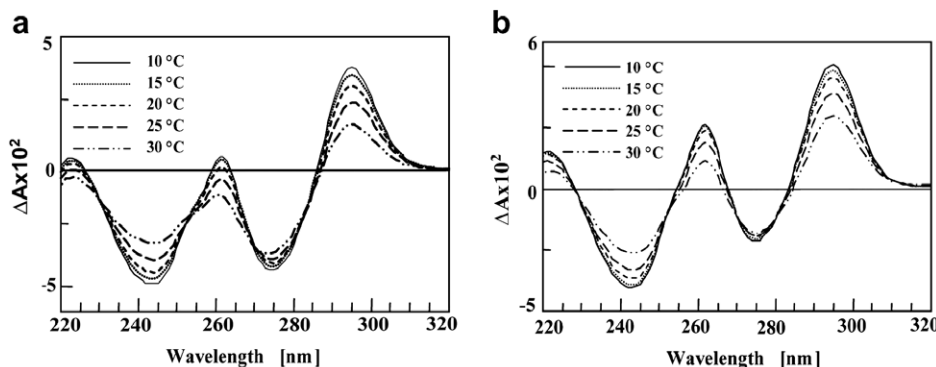
Figure 6. Differential UV spectra of **VII** (a) and **I** (b). Each differential profile is obtained by the subtraction of the spectrum registered at 65 °C from that obtained at each specific temperature. (10, 15, 20, 25, 30, and 35 °C). ON concentration: 1.0×10^{-5} M in physiological PBS.
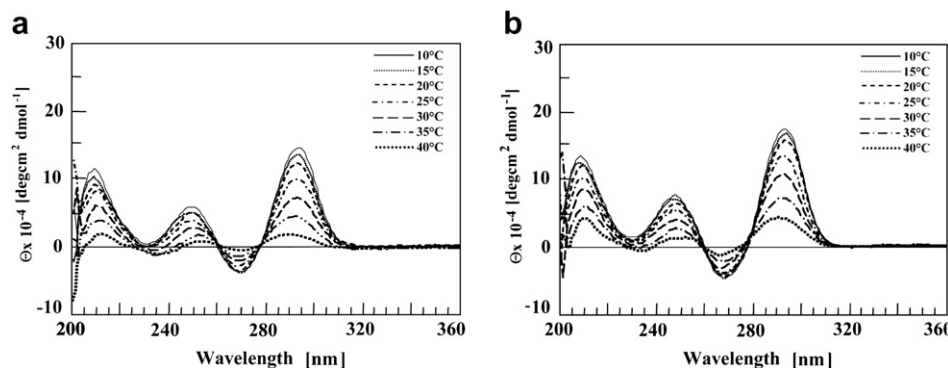
Figure 7. CD spectra of **VII** (a) and **I** (b) registered at various temperatures. ON concentration: 1.0×10^{-5} M in physiological PBS.
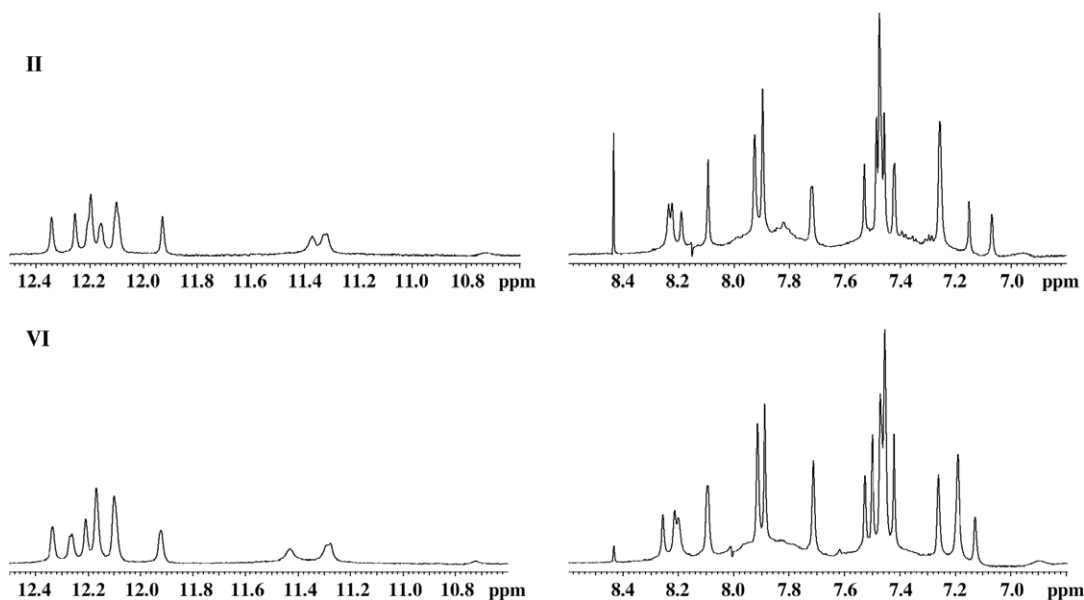
Figure 8. ^{1}H NMR imino (left) and aromatic (right) regions of **II** and **VI** (700 MHz, 2 °C).

of a T with the **T*** nucleoside produces two diastereomeric quadruplex-forming ONs. This effect is clearly observable in the upfield region of the ^{1}H NMR spectrum of some of the modified TBAs. In the ^{1}H NMR spectrum of **I** the methyl groups of thymines T4 and T13 resonate far away (0.98 and 1.03 ppm, respectively) from those of the other thymines (∼ 2.0 ppm), due to their particular position in the quadruplex folded structure (see later). Given that in all the modified TBAs reported here the aliphatic methyl group of the acyclic linker has been introduced, a total of three 3 H singlets were expected around 1.0 ppm. In almost all cases, however, more than three signals appear in that region. Particularly, for **III** and **VII** (Fig. 9) where the acyclic nucleoside substitutes T4 or T13, respectively, five and six signals, respectively, are clearly discernible. It is to be noted that by increasing the temperature above 45 °C the T4 and T13 methyl signals are downfield shifted, like those of the other thymines, whereas the linker methyl group resonates as a slightly split couple of singlets centered at 0.78 ppm as a consequence of the presence of the two diastereomeric random coil strands (data not shown).

In contrast to the other modified ONs, the ^{1}H NMR spectrum of **V** is very crowded, thus confirming that several conformations are simultaneously present in solution as suggested by the CD and UV experiments in which isoelliptical and isosbestic points are missing (not shown).

2.4. Prothrombin Time (PT) assay

It has been demonstrated that the unmodified **I** acts as a potent anticoagulant as a consequence of its ability to prevent the binding

of fibrinogen to the thrombin.[6,7] Differently from other thrombin inhibitors that bind to the catalytic site, the TBA binds the anionic exosite of the thrombin leaving unaltered the thrombin ability to cleave small chromogenic substrates. For this reason the inhibition constant (Ki) of TBA analogues cannot be determined by traditional methods, in which small chromogenic substrates are generally used. In these cases, the most commonly used methods to evaluate the anti-thrombin activity are the prothrombin time[6,20,23] (PT) (or INR or Quick time) assay and purified fibrinogen clotting assay.[6,24]

The PT assay is a routine diagnostic assay that evaluates in vitro the activation of extrinsic pathway of the coagulation cascade. It measures the time to clot upon the addition of excess of tissue factors to the plasma. The assay is most sensitive to the levels of the extrinsic pathway factor VII and "common" pathway factors I (fibrinogen), II (prothrombin), V, and X. The thromboplastin, the reagent used in the assay, consists of tissue factors and a mixture of phospholipids and calcium. Briefly, the thromboplastin induces a rapid conversion of plasmatic prothrombin into thrombin, which, in turn, converts fibrinogen into fibrin, forming the clot. In absence of a thrombin inhibitor, the time that elapses from the addition of thromboplastin to the formation of the clot represents the basal prothrombin time. When the assay is performed in presence of the unmodified aptamer **I** the binding of fibrinogen to the thrombin is inhibited and more time is required to form the clot. The TBAs analogues that prolong PT time more than unmodified **I** can be taken into account as better thrombin inhibitors.

Prothrombin times have been determined by using an automated coagulometer. To perform this assay we have used fresh citrated human plasma, thromboplastin, and a known concentration
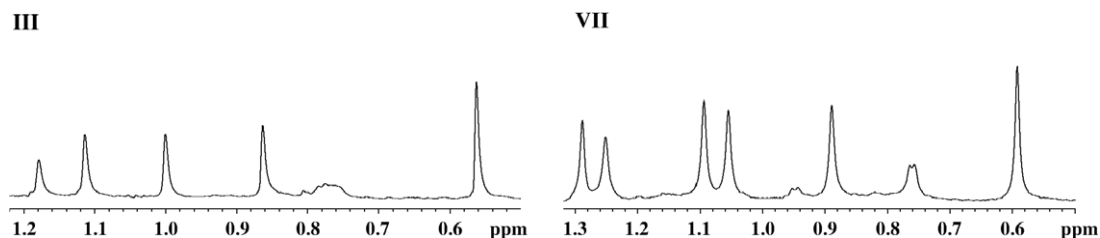

Figure 9. Upfield region of ^{1}H NMR spectra of **III** and **VII** showing the split of linker, T4, and T13 methyl signals (500 MHz, 25 °C).

of the ONs. The plasma has been incubated with 2 or 20 μM solutions of each ON at 37 °C. A set of experiments has been performed using different incubation times: 30 s, 2, 5, 10, 15, 30, and 60 min. After each incubation time, the clotting was initiated by addition of thromboplastin and the PT time was measured by analyzing the test on the coagulometer. Each PT measurement was produced in triplicate, so that, for each incubation times, an averaged PT time was calculated. Finally, for each ON, all the PT time values, measured at different incubation time, have been averaged in order to furnish the final PT value and its standard deviation. The results for unmodified **I**, reported in the Table 2, overlap with those previously obtained.[25]

The analysis of PT assays suggests that, although all modified TBAs have shown anti-thrombin activity at 20 μM, only **IV**, **VI**, and **VII** were significantly active at 2 μM (Table 2). The highest PT value was obtained for ON **IV** (Fig. 10) in which the modified nucleoside occupies the position 7 in the 15-mer sequence. The lowest PT values were obtained for ONs **II**, **III**, and **V** in which the modified nucleoside occupies the positions 3, 4, and 9, respectively. Interestingly the modified **V**, that shows the lowest thermal stability and the most complex ^{1}H NMR spectrum, induces a PT time similar to that observed for **II** and **III**.

2.5. Purified fibrinogen clotting time

The clotting of fibrinogen had been previously used to valuate the ability of TBA to bind thrombin and to inhibit the fibrinogen polimerization.[6,24] This assay is very similar to that of PT, but by avoiding the interaction among ONs and other blood components, it can be used to ascertain the direct relationship between the in vitro properties of the modified ONs, evaluated by PT assay, and their thrombin binding ability. To measure the clotting time in absence of any inhibitor (i.e., the basal clotting time), thrombin was added to a fibrinogen buffer solution, previously incubated at

37 °C for few minutes. The time required to form the fibrin clot has been measured by using a coagulometer. When TBA was added to the fibrinogen buffer solution, the clotting time was prolonged in a concentration-dependent manner. In order to compare the inhibitory activity of **I–VII** we have determined, for each of them, the concentration required to double the basal clotting time (Table 3).

Despite the experimental conditions used here were the same previously reported[6,24], the clotting time value obtained for unmodified **I** was about tenfold lower, whereas the basal clotting time perfectly overlapped with the previously reported findings. As shown in Table 3, **IV**, **VI**, and **VII** double the clotting time at lower concentration than **I**, whereas **II**, **III**, and **V** require a higher concentration. These results are comparable to those obtained by PT assay, implying that the in vitro activities of these ONs are directly associated to their thrombin binding ability.
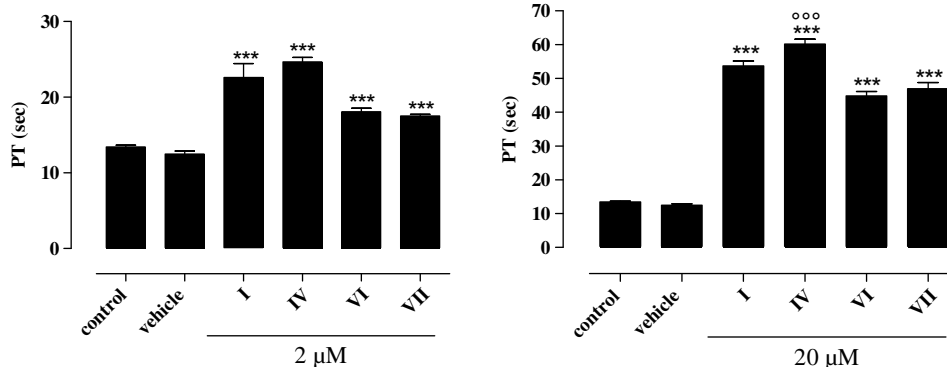
3. Discussion

The TBA (**I**) and its analogues (**II–VII**) show a similar behavior as far as the folding typology and the biological properties are concerned. As concerning CD analyses, the independence of molar ellipticity from the concentration has indicated that the folding is intramolecular when PBS is used as dissolving buffer. On the other hand, experiments performed in potassium buffer have shown that the molar ellipticity depends upon the concentration for all ONs, at both 10 and 30 °C. Vorlikôva and co-workers[21] have reported that the solution structure of TBA aptamer is bimolecular. However, our CD analyses confirm this datum only in potassium buffer, suggesting that the molecularity of the folded structures could be affected by the type of cations present in solution. Taking into account that

Table 2
Concentration-dependent response, following the ONs incubation (up to 60 min at 2 or 20 μM) with human plasma, on PT value expressed in seconds

ON	PT (2 μM)	PT (20 μM)
I	22.60 ± 1.83	53.68 ± 1.48
II	14.30 ± 0.31	35.15 ± 1.70
III	14.50 ± 0.20	32.28 ± 0.21
IV	24.67 ± 0.59	60.20 ± 1.38
V	13.23 ± 0.20	34.65 ± 2.01
VI	18.07 ± 0.47	44.83 ± 1.30
VII	17.50 ± 0.23	46.97 ± 1.83

The physiological value of human PT is 13.4 ± 0.22 s. PBS, used as vehicle, does not alter PT value (12.49 ± 0.39).

Table 3
Concentration required for each ON to double the fibrinogen clotting time

ON	[ON]$_{2t}$ nM (± 10)
I	175
II	238
III	250
IV	70
V	210
VI	78
VII	100

The basal time is determined by measuring the time required to form the clot in 200 μM of a fibrinogen buffer solution (2 mg in 1 mL of 20 mM Tris–acetate buffer containing 140 mM NaCl, 2.7 mM KCl, 1 mM MgCl$_2$, and 1 mM CaCl$_2$, pH 7.4) after the addition of 100 μM of buffer thrombin solution (at final concentration of 13 nM). Basal clotting time, averaged on six measurements, has been 27 ± 3 s. The ON concentration required to prolong the clotting time at final value of 57 ± 10 s was determined (see Section 5).

Figure 10. Incubation, up to 15 min, of **I**, **IV**, **VI**, and **VII** significantly and concentration-dependently increases the PT value. ***$p < 0.001$ vs vehicle, °°°$p < 0.001$ vs **I**. $n = 3$.

PBS mimes the blood salt composition, the intermolecular folding for which a highest potassium concentration is required should not be relevant from biological point of view.

The introduction of the acyclic nucleotide generates two diastereomeric strands in which the modified residue may assume an R or S configuration. Consequently, in PBS, the folding process of each modified ON produces two diastereomeric structures. However, the presence of isoelliptical and isosbestic points in thermal CD and differential UV spectra indicates that the two possible structures show similar arrangement and thermal stability.

The ^{1}H NMR spectra of all but **V** the modified ONs are similar to that of the unmodified one, besides the splitting of some imino and methyl signals. The presence of doubled signals in some regions could be confidentially attributable to the two diastereomeric structures.

The reported ^{1}H NMR of the TBA[12,13] showed in the upfield region two methyl signals at anomalous values (0.98 and 1.07 ppm, respectively) due to the methyl groups of T4 and T13 bases. The upfield shifts of these signals have been justified by the formation of a base pair stacked on the adjacent G-quartet in the monomolecular chair-like structure. It is noteworthy that in almost all cases a similar upfield shift for T4 and T13 methyl groups has been observed, thus suggesting that the structural arrangement is similar to that of TBA. The ^{1}H NMR of **V** appeared very crowded due to the presence of more than one structure in solution.

The in vitro biological properties of the new ONs have been valued by PT assay performed at 37 °C. Prior to the assay, each ON was annealed using the physiological PBS. In order to properly get insight into the structure-activity relationship, the spectroscopic experiments have been carried out in the same buffer. The UV and CD thermal experiments have shown that the T_m values of TBA and its analogues were lower or comparable to the temperature of the PT assay, pointing out that in physiological conditions they are present in solution mainly as unfolded ONs.

NMR and X-ray studies unequivocally assign to the TBA monomolecular quadruplex its ability to bind the thrombin with high specificity.[15,20] TBA-thrombin complex analyses evidence that the G-scaffold is fundamental for the complex stability.[11–15,20] As a direct consequence, it is suited to hold that every modification produced on the ON sequence (aimed at the improvement of specific properties such as the cellular permeability or the in vivo half-life) can be considered appropriate only if the resulting ONs improve or preserve the thermal stability of the folded chair-like quadruplex structure. However, our experimental data only partially agree with this overview, since a direct correlation between the structural stability and the biological activity is preserved mainly when the introduction of the modified nucleotide involves the TGT loop, whereas a more complex structure–activity relationship results in the case of TT loops modifications. Similar behavior was also found for other biologically active quadruplex-forming ON.[35]

Previous studies[13,24] had demonstrated that the substitution of the T7 with an abasic linker is associated with enhanced thrombin binding ability, whereas when the abasic linker replaces the T9 a loss of binding ability is observed. This is in agreement with the analyses of the structural data of the TBA-thrombin complex,[15] which have shown that the stacking of T9 and G8 on the adjacent G-quartet is important for the complex stability.

The same behavior has been observed for ONs **IV** and **V** in which the modification involves T7 and T9, respectively, thus confirming that the T9 and G8 stacking interactions are both required for the quadruplex stability and the thrombin binding activity. The enhancing of biological activity obtained for **IV** and other abasic site containing ONs[24] indicates that improved thrombin binding activity is achieved by increasing the flexibility at position 7 of TBA. This datum should be taken into account for the design of new TBA analogues.

As far as modifications involving the TT loops are concerned, no significant effect on quadruplex stability has been shown when the substitution concerns the positions 3 or 12. On the contrary, modified TBAs in which the substitution involves the position 4 or 13 have shown a lowering of the thermal stability. These results can be explained considering the NMR structure[12,13,20] in which T4 and T13 stack on adjacent G quartet and bind each other by a hydrogen bond. The introduction of an acyclic nucleotide at one of these two positions can induce the loss of stacking interactions and/or the loss of the H-bond, hence the diminution of T_m value.

A detailed analysis of the structure–activity relationship results in more difficulty because the X-ray structure of TBA–thrombin complex shows poor resolution about the TT loops positions.[11,12,15,20] As a consequence, the results obtained for **II** or **VII**, in which the acyclic nucleotide occupies the positions 3 and 13, respectively, were particularly intriguing. In fact, **VII** folds in a quadruplex structure having poor thermal stability, but among ONs in which TT loops have been modified; it shows the highest anti-thrombin activity. On the other hand, although **II** has kept the original thermal stability, it has partially lost the biological activity.

In order to shed light on our results and considering the temperature of the PT assay, the presence of an equilibrium between the folded form and the unfolded form, both likely being able to bind the thrombin, must be taken into account. In fact, Baldrich et al.[40] and Nagatoishi et al.[41] have demonstrated that thrombin is able to act as a molecular chaperon for the unfolded form of the TBA thus inducing the G-quadruplex formation. Furthermore, authors hypothesize that the recognition by "adaptive folding" could start by an interaction between the TT steps of the unfolded TBA and some hydrophobic residues of the protein. In this context, the recognition of the unfolded form by the protein could contribute significantly to the biological activity. Results concerning the PT assay (Table 2) and purified fibrinogen clotting assay (Table 3) obtained for ONs, in which TT loops have been modified, clearly indicate that modifications involving T3 or T4 result in lower biological activities than those concerning T12 or T13. These data seem to suggest that the chaperon process involves mainly the initial contact between thrombin and the TT loop flanking the 5′-end. The biological properties of **V** are comparable to that of **II** and **III**. It should take into account that its ability to fold into a chair-like quadruplex structure is dramatically compromised by the modification, as evidenced by its thermal stability being far lower than that of the other ONs.

Furthermore, more recently, it has been reported that TBA is able to bind both thrombin and prothrombin with similar affinity.[42] This means that any variation introduced in the sequence could interfere with the TBA ability to bind one or both the proteins. Prothrombin is an attractive target for novel anticoagulant agents since its inactivation determines the attenuation of thrombin generation preserving at the same time sufficient thrombin activity to permit hemostasis. For this reason, the binding affinity of modified ONs toward prothrombin should be evaluated for a more detailed valuation of in vitro effects. These studies will be successively performed by using the diastereomeric pure oligonucleotides whose synthesis is currently in progress in our laboratory.

4. Conclusion

In summary, the synthesis of a series of modified TBA analogues in which the T bases have been replaced, one at the time, by the new acyclic nucleotide N^1-(3-hydroxy-2-hydroxymethyl-2-methylpropyl)-thymine has been done. Each ON has been characterized by UV, CD, MS, and ^{1}H NMR experiments. The structural data have demonstrated that all ONs fold into quadruple helices whose

behavior is very similar to that of the unmodified counterpart. The spectroscopic data suggest that the molecularity of the formed quadruplex structure depends upon the nature of the cations present in the buffer. The biological activity of the new ONs has been valued by prothrombin time measurements and by purified fibrinogen clotting experiments. The modified ON containing the acyclic nucleotide at T7 position has shown a higher in vitro inhibitory activity than the unmodified sequence at the two tested concentrations of 2 and 20 μM.

Some new structure–activity relationships have been evidenced when the modification has involved the TT loops. Particularly, we suggest that important interactions must involve the TT loop located at 5′-end, most probably during the recognition of the unfolded form of TBA and the other ONs by the thrombin. At the best of our knowledge data concerning the events involved in the chaperon process have not been presented as yet. Since the TBA can be considered one of the most promising anticoagulant drugs, the full elucidation of its structure–activity relationships is particularly interesting. These results can contribute to the understanding of TBA-thrombin recognition process.

5. Experimental

5.1. UV spectroscopic temperature-dependent melting studies

Each ON, at a final concentration of 1.0×10^{-5} M, was dissolved in the potassium (100 mM KCl, 10 mM KH_2PO_4, pH 7.0) or sodium (PBS: 137 mM NaCl, 2.7 mM KCl, 10 mM NaH_2PO_4, pH 7.4) phosphate buffer.

All samples were submitted to the annealing procedure (heated at 90 °C and slowly cooled at room temperature).

The UV thermal stability experiments were carried out using a JASCO 530 spectrophotometer equipped with ETC-505 T temperature controller. Melting curves were obtained by monitoring the variation of absorbance at 295 nm from 10 to 80 °C. Two melting experiments for each ON were recorded, fixing the heating rate at 0.5 and 0.1 °C/min, respectively. The folding experiments were registered from 80 to 10 °C, using the same scan rates.

The differential absorption UV profiles were obtained by the subtraction of the spectrum registered at 65 °C from that obtained at each specific temperature (10, 15, 20, 25, 30, and 35 °C).

5.2. Circular dichroism spectra

The CD spectra were recorded from 200 to 360 nm (scanning rate: 100 nm/min; response: 16 s; bandwidth: 1.0 nm) on a JASCO 715 spectropolarimeter equipped with a PTC-348 temperature controller. All samples were previously submitted to the annealing procedure. Before the scan, the sample was equilibrated at the specific temperature (10 or 30 °C) for 30 min. Each CD profile was obtained by taking the average of three scans from which the spectrum of the buffer alone was subtracted.

To evaluate the dependence of molar ellipticity from the ON concentration in PBS and potassium buffer, three samples at different concentrations (1.0×10^{-4}, 1.0×10^{-5}, and 1.0×10^{-6} M) and three cuvettes having different path lengths (0.1, 0.5, and 1.0 cm), were used. The CD spectra at different temperatures have been registered using samples at 1.0×10^{-5} M in PBS or potassium buffer.

5.3. NMR experiments

^{1}H NMR data were collected on Varian Unity INOVA 500 and 700 MHz spectrometers equipped with broad-band inverse probes with z-field gradient and processed using Varian VNMR software package. 1D NMR spectra were acquired as 16,384 data points with a recycle delay of 1.0 s at temperatures in the range 2–50 °C. Data

sets were zero filled to 32,768 points prior to Fourier transformation and apodized with a shifted sine bell squared window function. Pulsed-field gradient DPFGSE[43,44] sequence was used for H_2O suppression. NMR samples **II–VII** were prepared in H_2O/D_2O (9:1, v/v) at a single strand concentration of approximately 0.5 mM, with a final salt concentration of 130 mM NaCl, 10 mM NaH_2PO_4, and 0.2 mM EDTA.

5.4. Prothrombin time (PT) assay

Human plasma samples were collected by venipuncture in presence of 0.1 volumes of 3.8% sodium citrate and fractionated by centrifugation at 2000 rpm for 5 min. PT time was measured by using Koagulab MJ Coagulation System with a specific kit RecombiPlas Tin HemosIL (Inst. Labs, Lexinton, USA). Briefly, this method relies on the high sensitivity thromboplastin reagent based on recombinant human tissue factors. The addiction of recombiplastin to the plasma in presence of calcium ions initiates the activation of extrinsic pathway converting the fibrinogen into fibrin, with a formation of solid gel. The procedure was performed according to the manufacturer's instructions. In our experimental protocol a time course of each ON or vehicle incubation with 100 μL of plasma at 37 °C has been performed. For the valuation of PT at 20 μM, in the apposite microtube, 2 μL of the corresponding ON solution (1.0×10^{-3} M in PBS) or vehicle was added. After 30 s, 1, 5, 15, 30, and 60 min of incubation, 200 μL of the kit solution containing recombiplastin was added with consequent activation of extrinsic pathway.

The PT at final ONs concentrations of 2 μM was determined using 2 μl of 1.0×10^{-4} M ON solution in PBS.

The PT measurement, for each incubation time, was produced in triplicate and the average value was calculated. Finally, all the PT time values measured at different incubation times were also averaged to furnish the final PT value and its standard deviation.

5.5. Purified fibrinogen clotting assay

ONs were incubated for 1 min at 37 °C in 200 μl of buffer (20 mM tris acetate, 140 mM NaCl, 2.7 mM KCl, 1 mM $MgCl_2$, 1 mM $CaCl_2$, pH 7.4) containing human fibrinogen (2 mg/mL). The human thrombin was dissolved in the same buffer and pre-equilibrated for 1 min at 37 °C. After this time 100 μl of thrombin was added to the solution containing the fibrinogen and the ON (the final concentration of thrombin was 13 nM). The time required to clot was measured using a Koagulab MJ Coagulation System. For each ON the experiment was performed at five different concentrations (20, 50, 100, 175, 200, and 300 nM), and the clotting time was determined by averaging six experiments for each ON concentration. The basal clotting time has been determined by measuring the clotting time in absence of any ONs. Clotting time versus [ON] was then reported to obtain a straight line, from which the concentration required to double the clotting, indicated as $[ON]_{2t}$, was obtained.

5.6. Synthesis

5.6.1. Reagent and equipment

Chemicals and anhydrous solvents have been purchased from Fluka–Sigma–Aldrich. TLCs were run on Merck silica gel 60 F_{254} plates, and compounds were visualized by $KMnO_4$ spraying reagent, and UV lamp. Silica gel chromatographies were performed by using Merck silica gel 60 (0.063–0.200 mm). API 2000 Analist NT Applied Biosystem ESI-MS spectrometer was used for analyses of the intermediates and the monomer. Reagents and phosphoramidites for DNA syntheses were purchased from Glen research. ON syntheses were performed on a PerSeptive Biosystem Expedite.

HPLC analyses and purifications were carried out by using Thermo-Finnigan Spectra SYSTEM P4000. To perform the purifications of the ONs a SAX 1000-8 Macherey–Nagel column was used. The desalting of ONs was performed by using molecular exclusion chromatography on BIORAD BioLogic LP system. To check the purification grade a Purospher® STAR RP-18 end-capped (5-μm) HPLC column was used. Mass spectrometric analyses of ONs were performed on Bruker Autoflex I MALDI-TOF mass spectrometer using piconilic/3-hydroxypiconilic acids mixture as the matrix.

5.6.2. 5-Hydroxymethyl-2,2,5-trimethyl-1,3-dioxane (1)

1,1,1-Tris(hydroxymethyl)ethane (41.63 mmol) was suspended in 50 mL of 2,2-dimethoxypropane. Pyridinium-p-toluene sulfonate (8.32 mmol) was added and the suspension was stirred at room temperature for 24 h under argon. Triethylamine was added to quench the reaction, and the solution was stirred for 30 min. The solvent was removed to leave a colorless liquid. The solid residue was chromatographed on silica gel eluted with 1:1 EtOAc/hexane to give a colorless liquid 1 (yield 67%), Rf 0.40 (1:1 EtOAc/hexane). ^{1}H NMR (CDCl$_3$) δ ppm 3.71–3.56 (dd, 4 H), 3.38 (s, 2H), 1.41 (s, 3H), 1.39 (s, 3H), 0.83 (s, 3H). ^{13}C NMR (CDCl$_3$) δ ppm 90.1, 68.2, 65.9, 37.0, 28.3,13.3. ESI MS m/z 161 [M+H]$^+$, 183 [M+Na]$^+$.

5.6.3. N^3-Benzoylthymine (2)

Thymine (8.55 mmol) was suspended in dry acetonitrile (10 mL) and dry pyridine (5 mL), and the mixture was cooled at 0 °C. Benzoyl chloride (19.1 mmol) was added and the reaction mixture was stirred at room temperature for 72 h, under argon. The mixture was evaporated under reduced pressure, and the residue was dissolved in dichloromethane and extracted with water (twice). The product was crystallized from dichloromethane giving colorless needles 2 (yield 85%), Rf 0.45 (9:1 CHCl$_3$/MeOH). ^{1}H NMR (CDCl$_3$) δ ppm 9.57 (br, 1H), 7.95 (d, 2H), 7.68 (t, 1H), 7.50 (t, 2H), 7.12 (s, 1H), 1.95 (s, 3H). ^{13}C NMR (CDCl$_3$) δ ppm 167.7, 162.1, 151.1, 142.1, 135.8, 132.1, 131.0, 129.9, 110.2, 18.7. 2D-NOESY NMR (CDCl$_3$) δ ppm: a NOE cross peak was found between H-6 (7.12) and N^{1}H (9.57). ESI MS m/z 231[M+H]$^+$, 253 [M+Na]$^+$.

5.6.4. 3-Benzoyl-5-methyl-1-[(2,2,5-trimethyl-1,3-dioxan-5-yl)-methyl]-pyrimidine-2,4(1H,3H)-dione (3)

2 (4.0 mmol), triphenylphosphine (6.0 mmol), di-$tert$-butyl azodicarboxylate (6.0 mmol) were suspended in 25 mL of dry dioxane; the resultant mixture was stirred and cooled to −20 °C and 1 was added. The reaction mixture was stirred at room temperature for 18 h under argon and a clear-yellow solution was obtained. The solution was concentrated under reduced pressure and the residue was purified by column chromatography on silica gel eluted with 95:5 Et$_2$O/CH$_2$Cl$_2$ to give a white solid 3 (yield 75%), Rf 0.59 (9:1 v/v CHCl$_3$/MeOH). ^{1}H NMR (CDCl$_3$) δ ppm 7.92 (d, 2H), 7.63 (t, 1H), 7.48 (t, 2H), 7.19 (s, 1H), 4.02 (s, 2H), 3.71–3.57 (dd, 4H), 1.97 (s, 3H), 1.47 (s, 3H), 1.46 (s, 3H), 0.79 (s, 3H). ^{13}C NMR (CDCl$_3$) δ ppm 167.7, 162.1, 151.1, 142.1, 135.8, 132.1, 131.0, 129.9, 110.2, 90.1, 67.0, 51.9, 37.0, 28.3, 18.7, 13.3. ESI MS m/z 373 [M+H]$^+$, 395 [M+Na]$^+$.

5.6.5. N^3-Benzoyl-N^1-(3-hydroxy-2-hydroxymethyl-2-methylpropyl)-thymine (4)

3 (2.83 mmol) was suspended in 9:1 MeOH/H$_2$O (50 mL), and 3 g of Dowex® 50WX8 (H$^+$) resin was added. The reaction mixture was slowly stirred at room temperature for 8 h up to complete dissolution of 3 and then a 0.5 M aqueous NaOH solution was added up to neutralization. The solution was concentrated under reduced pressure, obtaining 4 as a white solid (yield 98%); Rf 0.27 (9:1 CHCl$_3$/MeOH). ^{1}H NMR (CDCl$_3$) δ ppm 7.98 (d, 2H), 7.70 (t, 1H), 7.60 (s, 1H), 7.57 (t, 2H), 3.80 (s, 2H), 3.20 (m, 4H), 1.95 (s, 3H), 0.89 (s, 3H). ^{13}C NMR (CDCl$_3$) δ ppm 167.7, 162.1, 151.1, 142.1, 135.8, 132.1, 131.0, 129.9, 110.2, 65.8, 51.9, 42.0, 18.7, 13.3. ESI MS m/z 333 [M+H]$^+$, 355 [M+Na]$^+$.

5.6.6. N^3-Benzoyl-N^1-[3-methoxy(4,4′-dimethoxytrityl)-2-hydroxymethyl-2-methylpropyl]-thymine (5)

4 (1.54 mmol), 4,4′-dimethoxytrytyl chloride (1.23 mmol), and 4-dimethylaminopyridine (0.077 mmol) were dissolved in dry pyridine (10 mL) and dry acetonitrile (5 mL). The resulting solution was stirred for 1 h at room temperature under argon. Dry methanol was added to quench the reaction. After 30 min under stirring, the solution was concentrated under reduced pressure and the residue purified by column chromatography on silica gel eluted with 50:50:5 EtOAc/hexane/Et$_3$N to give a clear-yellow solid 5 (yield 45%), Rf 0.51 (1:1 v/v EtOAc/hexane). ^{1}H NMR (CDCl$_3$) δ ppm 7.90 (d, 2H), 7.65 (t, 1H), 7.48 (t, 2H), 7.40 (d, 2H), 7.38 (m, 3H), 7.35 (d, 4H), 7.12 (s, 1H), 6.85 (d, 4H), 3.95–3.75 (dd, 2H), 3.80 (s, 6H), 3.38–3.21 (m, 2H), 3.10–2.95 (m, 2H), 1.80 (s, 3H), 1.05 (s, 3H). ^{13}C NMR (CDCl$_3$) δ ppm 167.7, 162.1, 158.8, 151.1, 143.6, 142.1, 135.0, 135.5, 132.1, 131.0, 129.9, 129.5, 129.2, 128.4, 126.7, 113.4, 110.2, 94.5, 71.8, 65.9, 55.4, 51.2, 42.0, 18.7, 13.3. ESI MS m/z 635 [M+H]$^+$, 657 [M+Na]$^+$.

5.6.7. 3-[3-Benzoyl-5-methyl-2,4-dioxo-3,4-dihydropyrimidin-1(2H)-yl]-2-methoxy-(4,4′-dimethoxytrityl)-2-methylpropyl-2-cyanoethyl-diisopropylphosphoramidite (6)

5 (0.559 mmol) was dried in vacuo overnight before being dissolved in anhydrous CH$_2$Cl$_2$ (5 mL) and diisopropylethylamine (2.24 mmol, 4 equiv) under argon. To this solution, 2-cyanoethyl diisopropylchlorophosphoramidite was added (0.838 mmol, 1.5 equiv). After 20 min the reaction mixture was quenched by the addition of dry methanol, diluted with ethyl acetate (15 mL) and washed with 10% sodium carbonate solution (15 mL) and brine (15 mL). The organic layer was dried on magnesium sulfate and concentrated in vacuo. The residue was purified on silica gel column eluted with 80:10:10 v/v/v CH$_2$Cl$_2$:ethyl acetate:triethylamine. The fractions containing the product were collected and concentrated under $vacuum$ yielding a white foam 6 (82%), Rf 0.65 (97:3 CHCl$_3$/MeOH). ^{1}H NMR (CDCl$_3$) δ ppm 7.90 (d, 2H), 7.65 (t, 1H), 7.48 (t, 2H), 7.40 (d, 2H), 7.38 (m, 3H), 7.35 (d, 4H), 7.12 (s, 1H), 6.85 (d, 4H), 3.95–3.80 (m, 2H), 3.75 (s, 6H), 3.70 (m, 2H), 3.60 (m, 2H), 3.55 (m, 2H) 3.39-3.02 (m, 2H), 2.60–2.45 (t, 2H), 1.80 (s, 3H), 1.09 (s, 12H) 1.05 (s, 3H). ^{13}C NMR (CDCl$_3$) δ ppm 163.3, 158.7, 150.6, 141.8, 135.0, 130.6, 130.4, 129.3, 129.2, 128.4, 128.1, 128.1, 127.0, 113.4, 110.1, 94.5, 66.1, 55.4, 54.2, 51.2, 43.3, 42.0, 24.7, 20.7, 18.7, 13.3. ESI MS m/z 835.7 [M+H]$^+$, 857.7 [M+Na]$^+$.

5.7. Synthesis of oligomers

TBA and analogues were synthesized by using standard solid-phase DNA chemistry on controlled pore glass (CPG) support following the β-cyanoethyl phosphoroamidite method.[28] The oligomers were detached from the support and deprotected by treatment with an aqueous ammonia solution (33%) at 55 °C overnight. The combined filtrates and washings were concentrated under reduced pressure, dissolved in H$_2$O, and purified by HPLC using an anionic exchange column eluted with a linear gradient (from 0% to 100% B in 30 min) of phosphate buffer at pH 7.0 (A: 20 mM NaH$_2$PO$_4$ aqueous solution containing 20% CH$_3$CN; B: 1 M NaCl, 20 mM NaH$_2$PO$_4$ aqueous solution containing 20% CH$_3$CN). The oligomers were successively desalted by molecular exclusion chromatography on Biogel P-2 fine. The purity was checked on HPLC by using reverse phase column (C-18 Purospher STAR, Merck) and electrophoresis on 20% denaturing polyacrylamide gel containing 7 M urea. The concentrations of the samples used in CD and UV experiments were determined by measuring absorbance at

260 nm at 80 °C using the extinction coefficients calculated according to Gray et al. method.[45] The extinction coefficient of the modified acyclic nucleotide has been assumed equal to that of the unmodified thymidine.

MALDI-TOF MS m/z (calcd. 4738 [M−H]⁻, 4761 [M−2 H+Na]⁻) 4736 (**II**, [M−H]⁻), 4736 (**III**, [M−H]⁻), 4735 (**IV**, [M−H]⁻), 4734 (**V**, [M−H]⁻), 4763 (**VI**, [M−2H+Na]⁻), 4762 (**VII**, [M−2H+Na]⁻).

Acknowledgements

References and notes

1. Bode, W. *Blood Cell. Mol. Dis.* **2006**, *36*, 122–130.
2. Dahlback, B. *J. Int. Med.* **2005**, *257*, 209–223.
3. Colman, R. W.; Hirsh, J.; Marder, V. J.; Clowes, A. W. In *Hemostasis and Thrombosis: Basic Principles and Clinical Practice*, 4th ed.; Lippincott Williams and Wilkins: Philadelphia, 2004; pp 17–20.
4. Weitz, J. I.; Hirsh, J. *Chest* **2001**, *119*, 95S–107S.
5. Di Nisio, M.; Middeldorp, S.; Buller, H. R. *N. Engl. J. Med.* **2005**, *353*, 1028–1040.
6. Bock, L. C.; Griffin, L. C.; Latham, J. A.; Vermaas, E. H.; Toole, J. J. *Nature* **1992**, *355*, 564–566.
7. Griffin, L. C.; Tidmarsh, G. F.; Bock, L. C.; Toole, J. J.; Leung, L. L. K. *Blood* **1993**, *81*, 3271–3276.
8. Tsiang, M.; Gibbs, C. S.; Griffin, L. C.; Dunn, K. E.; Leung, L. L. K. *J. Biol. Chem.* **1995**, *270*, 19370–19376.
9. Paborsky, L. R.; McCurdy, S. N.; Griffin, L. C.; Toole, J. J.; Leung, L. L. K. *J. Biol. Chem.* **1993**, *268*, 20808–20811.
10. Tasset, D. M.; Kubik, M. F.; Steiner, W. *J. Mol. Biol.* **1997**, *272*, 688–698.
11. Padmanabhan, K.; Padmanabhan, K. P.; Ferrara, J. D.; Sadler, J. E.; Tulinsky, A. *J. Biol. Chem.* **1993**, *268*, 17651–17654.
12. Macaya, R. F.; Schultze, P.; Smith, F. W.; Roe, J. A.; Feigon, J. *Proc. Natl. Acad. Sci. U.S.A* **1993**, *90*, 3745–3749.
13. Wang, K. Y.; McCurdy, S.; Shea, R. G.; Swaminathan, S.; Bolton, P. H. *Biochemistry* **1993**, *32*, 1899–1904.
14. Wang, K. Y.; Krawczyk, S. H.; Bischofberger, N.; Swaminathan, S.; Bolton, P. H. *Biochemistry* **1993**, *32*, 11285–11292.
15. Padmanabhan, K.; Tulinsky, A. *Acta Crystallogr.* **1996**, *D52*, 272–282.
16. Tuerk, C.; Gold, L. *Science* **1990**, *249*, 505–510.
17. Abelson, J. *Science* **1990**, *249*, 488–489.
18. Nimjee, S. M.; Rusconi, C. P.; Sullenger, B. A. *Annu. Rev. Med.* **2005**, *56*, 555–583.
19. Mao, X.; Gmeiner, W. H. *Biophys. Chem.* **2005**, *113*, 155–160.
20. Kelly, J. A.; Feigon, J.; Yeates, T. O. *J. Mol. Biol.* **1996**, *256*, 417–422.
21. Fialová, M.; Kypr, J.; Vorlìcková, M. *Biochem. Biophys. Res. Commun.* **2006**, *344*, 50–54.
22. He, G.-X.; Krawczyk, S. H.; Swaminathan, S.; Shea, R. G.; Dougherty, J. P.; Terhorst, T.; Law, V. S.; Griffin, L. C.; Coutré, S.; Bischofberger, N. *J. Med. Chem.* **1998**, *41*, 2234–2242.
23. He, G.-X.; Williams, J. P.; Postich, M. J.; Swaminathan, S.; Shea, R. G.; Terhorst, T.; Law, V. S.; Mao, C. T.; Sueoka, C.; Coutré, S.; Bischofberger, N. *J. Med. Chem.* **1998**, *41*, 4224–4231.
24. Krawczyk, S. H.; Bischofberger, N.; Griffin, L. C.; Law, V. S.; Shea, R. G.; Swaminathan, S. *Nucleosides Nucleotides Nucleic Acids* **1995**, *14*, 1109–1116.
25. Martino, L.; Virno, A.; Randazzo, A.; Virgilio, A.; Esposito, V.; Giancola, C.; Bucci, M.; Cirino, G.; Mayol, L. *Nucleic Acids Res.* **2006**, *34*, 6653–6662.
26. Merle, Y.; Bonneil, E.; Merle, L.; Sage, J.; Szmezö, A. *Int. J. Biol. Macromol.* **1995**, *17*, 239–246.
27. Marshalko, S. J.; Schweitzer, I. B.; Beardsley, G. P. *Biochemistry* **1995**, *34*, 9235–9248.
28. Zhang, L.; Periz, A.; Meggers, E. V. *J. Am. Chem. Soc.* **2005**, *127*, 4174–4175.
29. Joyce, G. F. *Nature* **2002**, *418*, 214–221.
30. Mitsunobu, O. *Synthesis* **1981**, *1*, 1–28.
31. Di Grandi, M. J.; Tilley, J. W. *Tetrahedron Lett.* **1996**, *37*, 4327–4330.
32. Cruickshank, K. A.; Jiricny, J.; Reese, C. B. *Tetrahedron Lett.* **1984**, *25*, 681–684.
33. Park, K. H.; Yoon, Y. J.; Lee, S. G. *Tetrahedron Lett.* **1994**, *35*, 9737–9740.
34. Sinha, N. D.; Biernat, J.; McManus, J.; Koster, H. *Nucleic Acids Res.* **1984**, *12*, 4539–4557.
35. Dapić, V.; Abdomerović, V.; Marrington, R.; Peberdy, J.; Rodger, A.; Trent, J. O.; Bates, P. J. *Nucleic Acids Res.* **2003**, *31*, 2097–2107.
36. Mergny, J.-L.; Phan, A.-T.; Lacroix, L. *FEBS Lett.* **1998**, *435*, 74–78.
37. Mergny, J.-L.; Li, J.; Lacroix, L.; Amrane, S.; Chaires, J. B. *Nucleic Acids Res.* **2005**, *33*, e138/1–e138/6.
38. Saccà, B.; Lacroix, L.; Mergny, J.-L. *Nucleic Acids Res.* **2005**, *33*, 1182–1192.
39. Gros, J.; Rosu, F.; Amrane, S.; De Cian, A.; Gabelica, V.; Lacroix, L.; Mergny, J.-L. *Nucleic Acids Res.* **2007**, *35*, 3064–3075.
40. Baldrich, E.; O'Sullivan, C. K. *Anal. Biochem.* **2005**, *341*, 194–197.
41. Nagatoishi, S.; Tanaka, Y.; Tsumoto, K. *Biochem. Biophys. Res. Commun.* **2007**, *352*, 812–817.
42. Kretz, C. A.; Stafford, A. R.; Fredenburgh, J. C.; Weitz, J. *J. Biol. Chem.* **2006**, *281*, 37447–37485.
43. Hwang, T. L.; Shaha, A. J. *J. Magn. Res.* **1995**, *A112*, 275–279.
44. Dalvit, C. *J. Biomol. NMR* **1998**, *11*, 437–444.
45. Gray, D. M.; Hung, S. -H.; Johnson, K. H. *Methods Enzymol.* **1995**, *246*, 19–34.